Received: 17 October 2023 | Revised: 20 December 2023 | Accepted: 2 January 2024

DOI: 10.1111/pce.14817

ORIGINAL ARTICLE

Plant, Cell & Environment | WILEY

A complex array of factors regulate the activity of *Arabidopsis thaliana* δ[1]-pyrroline-5-carboxylate synthetase isoenzymes to ensure their specific role in plant cell metabolism

Giuseppe Forlani[1] | Giuseppe Sabbioni[1] | Simone Barera[1] | Dietmar Funck[2]

[1]Department of Life Science and Biotechnology, University of Ferrara, Ferrara, Italy

[2]Department of Chemistry, University of Konstanz, Konstanz, Germany

Correspondence
Giuseppe Forlani, Department of Life Science and Biotechnology, University of Ferrara, via L. Borsari 46, I-44121 Ferrara, Italy.
Email: flg@unife.it

Funding information
National Recovery and Resilience Plan; University of Ferrara; Italian Ministry of University and Research

Abstract

The first and committed step in proline synthesis from glutamate is catalyzed by δ[1]-pyrroline-5-carboxylate synthetase (P5CS). Two P5CS genes have been found in most angiosperms, one constitutively expressed to satisfy proline demand for protein synthesis, the other stress-induced. Despite the number of papers to investigate regulation at the transcriptional level, to date, the properties of the enzymes have been subjected to limited study. The isolation of *Arabidopsis thaliana* P5CS isoenzymes was achieved through heterologous expression and affinity purification. The two proteins were characterized with respect to kinetic and biochemical properties. *At*P5CS2 showed K_M values in the micro- to millimolar range, and its activity was inhibited by $NADP^+$, ADP and proline, and by glutamine and arginine at high levels. Mg^{2+} ions were required for activity, which was further stimulated by K^+ and other cations. *At*P5CS1 displayed positive cooperativity with glutamate and was almost insensitive to inhibition by proline. In the presence of physiological, nonsaturating concentrations of glutamate, proline was slightly stimulatory, and glutamine strongly increased the catalytic rate. Data suggest that the activity of *At*P5CS isoenzymes is differentially regulated by a complex array of factors including the concentrations of proline, glutamate, glutamine, monovalent cations and pyridine dinucleotides.

KEYWORDS
amino acid metabolism, cooperative enzyme, feedback and product inhibition, isoenzymes, P5C synthetase, posttranslational regulation, proline synthesis, pyridine nucleotide pools

1 | INTRODUCTION

Plant genetic improvement for increased stress tolerance is required to ensure high crop productivity and suffice the needs of a rapidly growing world population, also taking into account the threat represented by the ongoing climate changes (Raza et al., 2019). Under water stress conditions, plants achieve osmotic compensation through the accumulation of the so-called compatible osmolytes (Ghosh et al., 2021), among which the amino acid proline is the most widespread (Verbruggen & Hermans, 2008). However, in several instances, the intracellular concentration of proline seems not high enough to contribute significantly to osmotic adjustment under stress (Forlani, Bertazzini, et al., 2019). In addition, proline is synthesized and accumulated not only in response to hyperosmotic stress but also following the exposure to cold and frost, heavy metals or pathogen attack (Hayat et al., 2012). To explain such a complex pattern of

induction, other possible beneficial effects of proline accumulation have been evoked, ranging from reactive oxygen species (ROS) scavenging to stabilization of membranes and enzymes, from balancing of the redox status of the cell to induction of antioxidant defences (Forlani, Trovato, et al., 2019).

In most cases, stress-induced proline accumulation relies upon an increase in its biosynthetic rate (Trovato et al., 2019). In plants, proline biosynthesis occurs through a short, two-step pathway (Supporting Information S1: Figure S1). At first, the bifunctional enzyme δ^1-pyrroline-5-carboxylate (P5C) synthetase (P5CS), bearing both γ-glutamyl kinase (GK, EC 2.7.2.11) and NADPH-dependent γ-glutamyl phosphate reductase (GPR, EC 1.2.1.41) activity, produces glutamate-5-semialdehyde (Rai & Penna, 2013). In solution, the latter spontaneously cyclizes to P5C, which is in turn reduced to proline by P5C reductase (P5CR, EC 1.5.1.2) using either NADH or NADPH as the electron donor (Forlani, Makarova, et al., 2015). Correlative evidence supported the occurrence in some plants of a biosynthetic route from ornithine via ornithine-δ-aminotransferase (EC 2.6.1.13) (Fichman et al., 2015), but this pathway is unlikely to contribute to proline synthesis in thale cress (*Arabidopsis thaliana*) (Winter et al., 2015). Only recently, we characterized AtDin11 as an enzyme with arginine-5-hydroxylase activity, which initiated nonenzymatic P5C formation by the decay of 5-hydroxyarginine (Funck et al., 2023). However, this activity is insufficient to replace P5CS activity, as evidenced by the lethality of pollen lacking P5CS expression (Funck et al., 2012; Mattioli et al., 2012).

In many higher plants, two *P5CS* paralogs have been identified, whose duplication occurred independently in several taxonomic groups (Rai & Penna, 2013; Turchetto-Zolet et al., 2009). These isoenzymes, referred to as P5CS1 and P5CS2, showed nonoverlapping roles, with varying temporal and spatial expression patterns. In rice (*Oryza sativa*), *P5CS1* was induced by stress conditions, such as the exposure to salt, dehydration and cold. *P5CS2* expression was found in mature plant parts, yet it was also induced by salt and mannitol treatments (Forlani, Bertazzini, Zarattini, & Funck, 2015; Rai & Penna, 2013). In *A. thaliana*, more distinct functions seem evident. The analysis of GFP-fused proteins suggested partial chloroplastic localization of PCS1, whereas P5CS2:GFP was predominantly found in the cytosol (Székely et al., 2008). However, more recent data conclusively demonstrated a cytosolic localization of both isoenzymes (Funck et al., 2020). *AtP5CS1* is moderately expressed in most plant organs and strongly induced under stress conditions, whereas *AtP5CS2* is transcribed to high levels in actively dividing cells (Strizhov et al., 1997; Székely et al., 2008). Knockout *p5cs1* mutants were hypersensitive to excess salt or high osmolarity and showed reduced proline synthesis and increased ROS accumulation under stress (Sharma et al., 2011; Székely et al., 2008). In contrast, *p5cs2* mutations caused embryo abortion during late stages of seed development but hardly affected proline accumulation under stress (Funck et al., 2020; Székely et al., 2008). Overall, *At*P5CS1 has therefore been identified as the major contributor to stress-induced proline synthesis, whereas *At*P5CS2 plays a fundamental role in embryo development and growth. Consistently, the occurrence of a wide and different array of putative transcription factor binding sites was found in the promoters of the two paralogs (Fichman et al., 2015; Zarattini & Forlani, 2017).

Contrary to the large amount of information available on *P5CS* gene expression in different plant species and tissues, during development and in response to environmental signals, little is known about the biochemical features of P5CS and the occurrence of posttranslational regulatory mechanisms. The activity of recombinant P5CS isolated from *Vigna aconitifolia* showed 50%-inhibition at 6 mM proline (Hu et al., 1992) and K_M values for glutamate and ATP of 3.6 mM and 2.7 mM, respectively (Zhang et al., 1995). Alignment of the *Va*P5CS sequence with other plant P5CS sequences suggests that it may be derived from a truncated cDNA because it lacks a highly conserved region at the C-terminus (Supporting Information S1: Figure S2). Two amino acid residues, Asp_{126} and Phe_{129}, which are highly conserved among plant P5CS enzymes, were found to be involved in feedback inhibition of *Va*P5CS by proline (Zhang et al., 1995). More recently, we described the functional properties of P5CS2 from rice (Sabbioni et al., 2021). The enzyme showed substrate affinity in the millimolar range, was stimulated by chlorides and inhibited by proline, arginine, ornithine and glutamine. Results supported some long-lasting hypotheses linking modulation of proline biosynthesis with either the nitrogen (Delauney et al., 1993; Delauney & Verma, 1993) or the redox status of the cell (Giberti et al., 2014; Sharma et al., 2011; Shinde et al., 2016). However, despite several attempts the purification of the other isoenzyme was not achieved, preventing a comparison of the properties of the two rice paralogs. Here we report on the heterologous expression, purification and biochemical characterization of the two P5CS isoenzymes from *A. thaliana*. Despite their high sequence identity (Supporting Information S1: Figure S2), the two proteins showed different functional features and dissimilar posttranslational regulative mechanisms, suggesting activity modulation in vivo by a complex array of factors including the concentrations of related amino acids, cations and pyridine dinucleotides.

2 | MATERIALS AND METHODS

2.1 | Chemicals

Unless indicated otherwise, chemicals were purchased from Sigma-Aldrich. NADPH was obtained from Carlo Erba Reagents. DL-P5C was synthesized by the periodate oxidation of δ-*allo*-hydroxylysine and purified by cation exchange chromatography, as described (Forlani & Funck, 2020).

2.2 | Cloning, heterologous expression and affinity purification

The coding sequence of *At*P5CS1 was amplified by PCR from ABRC clone U14433 and inserted by Gibson assembly into a pET24 derivative, introducing an N-terminal His_6-tag followed by a tobacco etch virus (TEV) protease cleavage site. An equivalent construct for *At*P5CS2 did not yield sufficient amounts of soluble protein.

Therefore, the coding sequence of *At*P5CS2 without stop codon was amplified by PCR from ABRC clone G2E1 and inserted by Gibson assembly into NdeI/XhoI-linearized pET24a, yielding an expression construct for *At*P5CS2 with C-terminal His_7-tag.

For heterologous expression, *Escherichia coli* SoluBL21 cells (Invitrogen), made competent by the calcium chloride method, were transformed with either vector. The cells were harvested 20–22 h after inducing the expression of P5CS by the addition of 1 mM isopropyl-β-D-thiogalattopyranoside (IPTG), lysed at 4°C in a pre-cooled mortar with 2 g g^{-1} aluminium oxide (150 mesh, Sigma 267740) and resuspended in 20 mL g^{-1} of extraction buffer (50 mM Na phosphate buffer, pH 7.5, containing 200 mM NaCl, 0.5 mM dithiothreitol [DTT] and 20 mM imidazole). The His-tagged proteins were purified from clarified extracts by affinity chromatography with His-SpinTrap columns (0.1 mL bed volume; Cytiva). After extensive washing with extraction buffer, P5CS isoenzymes were eluted with step-wise imidazole gradients in extraction buffer (Supporting Information S1: Figures S3 and S4).

For activity assays, the purified enzyme was routinely diluted with assay buffer (50 mM Tris-HCl, pH 7.4). When aiming at the assessment of the effect of a specific anion or cation on enzyme activity, purified samples were desalted immediately before the use by passage through a Bio-Gel P6DG (Bio-Rad) column equilibrated with either 10 mM Tris-HCl buffer, pH 7.4, or 10 mM Na phosphate buffer, pH 7.5, both containing 1 mM DTT.

2.3 | Enzyme assay

P5CS activity was measured at 30°C as the Glu- and ATP-dependent oxidation of NADPH in the presence of 100 mM Tris-HCl buffer, pH 7.4, as previously described (Sabbioni et al., 2021), with minor modifications. For *At*P5CS1, the assay mixture contained 250 mM L-Glu, 2.5 mM ATP, 0.5 mM NADPH and 5 mM $MgCl_2$. For *At*P5CS2, the assay mixture contained 50 mM L-Glu, 5 mM ATP, 0.5 mM NADPH and 2.5 mM $MgCl_2$. A limiting amount of enzyme (from 0.1 to 0.4 nkat) was added to the prewarmed mixture in a final volume of 0.2 mL in 96-microwell plates, and the decrease in absorbance at 340 nm was determined at 30-s intervals for up to 10 min using a Ledetect plate reader (Labexim). Unspecific NADPH oxidation rates were determined in parallel blanks from which Glu had been omitted. Activity was determined from the initial linear rate, with the assumption of an extinction coefficient for NADPH of 6220 M^{-1} cm^{-1}. Protein concentration was determined by the Coomassie Blue method (Bradford, 1976), with bovine serum albumin as standard.

2.4 | Electrophoresis

Samples were mixed with the same volume of 2× treatment buffer (125 mM Tris-HCl buffer, pH 6.8, containing 4% [w/v] SDS, 20% [v/v] glycerol, 10% [v/v] β-mercaptoethanol) and treated for 5 min at 100°C. Denatured sample aliquots were subjected to polyacrylamide gel electrophoresis (5% stacking, 8 or 10% separating gel, 29:1 acrylamide-bisacrylamide) at 8 mA. Gels were stained for protein with Coomassie Blue R250.

2.5 | Statistical analysis

Each sample was carried out in triplicate (technical replications). Each determination was repeated with at least three different enzyme preparations (biological replications). Unless otherwise specified, presented data refer to a single enzyme preparation and are means ± standard error over technical replicates. Linear and nonlinear regressions of data, as well as kinetic constant values, concentrations causing 50% inhibition (IC_{50}) of P5CS activity and their confidence intervals were computed using Prism 6 for Windows, version 6.03 (GraphPad Software).

3 | RESULTS

3.1 | *At*P5CS2 requires Mg^{2+} ions for activity and is stimulated by the presence of cations, mainly K^+

The heterologous expression in *E. coli* of the isoenzyme that is believed to provide cells with the amounts of proline needed for protein synthesis required a thorough optimization of the experimental conditions, including host strain, expression plasmid, position of the affinity tag, growth temperature and time of induction. In most cases, even though the protein was produced to significant amounts that were clearly evident upon sodium dodecyl sulphate–polyacrylamide gel electrophoresis (SDS-PAGE) analysis of total extracts, very low activity levels were found in the supernatant following centrifugation of cell-free extracts, and the corresponding band was not evident when the soluble fraction was analyzed, suggesting almost complete sequestering of the plant enzyme in inclusion bodies. Only the adoption of low growth temperatures (<24°C) and long incubation periods following the addition of IPTG (>20 h) allowed the attainment of significant activity levels in crude extracts. Affinity chromatography of the His-tagged protein resulted in low yields (Supporting Information S1: Figure S3), with more than 90% of the heterologous protein present in the flow-through. Moreover, the purified enzyme was remarkably unstable, with an almost complete loss of activity after 24 h at 4°C. The addition of the most commonly used protectants to the storage buffer, such as glycerol, reducing agents, protease inhibitors or ethylenediaminetetraacetic acid (EDTA), did not significantly improve enzyme stability (not shown). As a consequence, small amounts of the protein were purified each day and used for the assessment of the functional properties of the enzyme within a few hours after isolation.

When the glutamate and ATP-dependent oxidation of NADPH was measured using the purified preparations, low activity levels were found in the absence of further additions. Contrary to P5CS2 from rice (Sabbioni et al., 2021), activity was strongly increased by the presence of Mg^{2+} ions in the 10^{-4} to 10^{-3} M range, with maximal

effect at 2–5 mM, resulting in a 10-fold stimulation of the basal level (Figure 1a). In the absence of Mg^{2+}, activity was completely abolished by millimolar levels of EDTA, suggesting an absolute requirement for Mg^{2+}, which could not be replaced by monovalent cations such as K^+. In the presence of saturating Mg^{2+} levels, Ca^{2+} ions at concentrations exceeding 1 mM were found inhibitory. Interestingly, enzyme activity was stimulated by the addition of several salts at millimolar levels, with KCl being the most effective (Figure 1b). The comparison of the effect of different cations, all added as chlorides, and that of different anions, provided as Na^+ or K^+ salts (Figure 1b,c, respectively), pointed out a general stimulatory effect of cations in the 1–100 mM range and enzyme inhibition by anions over 100 mM. The effect of K^+ was noteworthy, being already evident at concentrations as low as 0.5 mM and caused a 2.5-fold stimulation of the catalytic rate at the optimal concentration of 100 mM.

3.2 | *At*P5CS2 shows a low catalytic constant and is subjected to product inhibition by $NADP^+$ and ADP

The specific activity level of purified *At*P5CS2 under standard assay conditions was 41.8 ± 3.4 nkat mg^{-1} (n = 30). When a single substrate concentration was varied for the activity measurement while maintaining the other two at a fixed, nearly saturating level, the enzyme

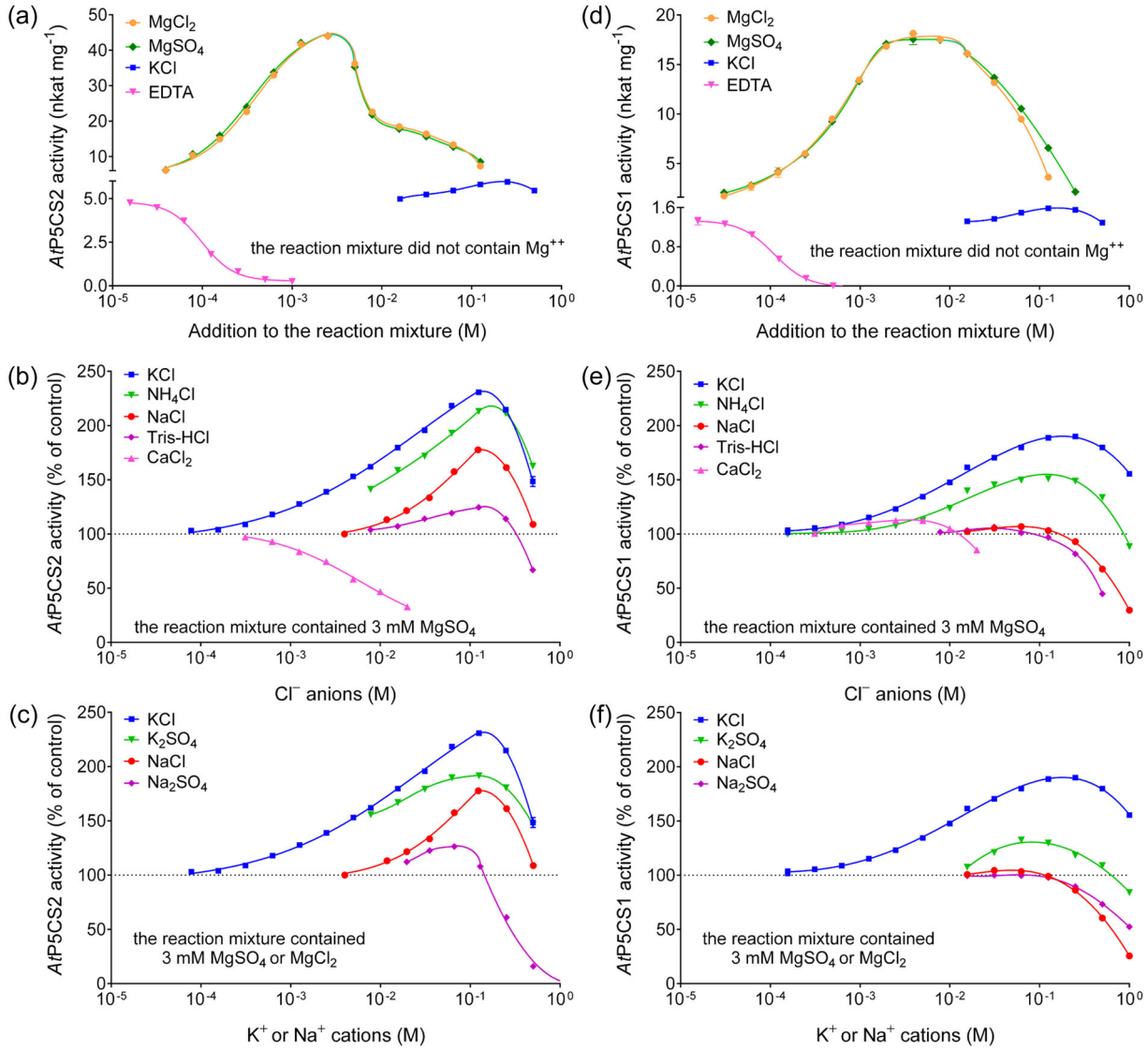

FIGURE 1 Effect of anions and cations on the activity of *Arabidopsis thaliana* P5CS isoenzymes. The purified proteins were assayed in a reaction mixture lacking Mg^{2+} ions, supplemented with increasing concentrations of $MgCl_2$, $MgSO_4$, KCl or EDTA, and the resulting specific activity was measured (a) and (d) for *At*P5CS2 and *At*P5CS1, respectively. In the presence of a saturating concentration of $MgSO_4$, the assay was carried out adding increasing concentrations of various chlorides. The resulting activity was expressed as percent of the value found in the absence of the latter (b) and (e). The assay was alternatively performed in the presence of K^+ or Na^+ chlorides or sulphates, using a Mg^{2+} salt with a different anion. Also in this case the results were expressed as percent of the value found in the absence of K^+ or Na^+ salts (c) and (f). EDTA, ethylenediaminetetraacetic acid; P5CS, δ^1-pyrroline-5-carboxylate synthetase.

showed typical Lineweaver–Burk kinetic responses (Figure 2). The calculated V_{MAX} values were around 45–50 nkat mg^{-1}. Taking into account a molecular mass of the heterologous protein of 81 kDa for a single monomer, this corresponds to a catalytic constant of about 4 s^{-1}. The K_M values were 3.9 mM for glutamate (Figure 2a), 0.32 mM for ATP (Figure 2b) and 32 μM for NADPH (Figure 2c). The use of NADH as the electron donor did not result in detectable activity rates.

Since previous studies on P5CS2 from rice had shown the occurrence of product inhibition (Sabbioni et al., 2021), the effect of increasing concentrations of $NADP^+$, ADP, Pi and P5C on enzyme activity was investigated. $NADP^+$ was particularly inhibitory, with a concentration causing 50% inhibition (IC_{50}) under standard assay conditions of 0.45 mM. When the concentration of NADPH in the reaction mixture was lowered, the effect increased, suggesting competitive inhibition (Figure 3a). This was confirmed by a kinetic analysis, showing a K_I value of 54 μM (Figure 3b) and a resulting K_I/K_M ratio of 1.7. Also ADP was found inhibitory in the 1–10 mM range, and the IC_{50} value decreased when the concentration of ATP in the assay was reduced (Figure 4a). The kinetic analysis confirmed an inhibition of competitive type with respect to the substrate (Figure 4b) but showed a K_I value of 1.9 mM, corresponding to a relatively high K_I/K_M ratio (5.9). Phosphate was also inhibitory, but only at concentrations exceeding 10 mM, and its effect did not appear of competitive type with respect to ATP (Figure 4c). The addition of micro- to millimolar concentrations of P5C did not inhibit *At*P5CS2 activity (Figure 5a). On the contrary, a slight stimulation was evident. However, this effect could depend on the carry-over of ions and not on P5C itself. In fact, DL-P5C is stable only in a strongly acidic environment and is obtained as a 50 mM solution in 1 M HCl that is neutralized just before the use. Therefore, this effect might most likely depend on the presence of the amount of Tris base (whose stimulatory action is shown in Figure 1b) that was used to correct the pH of the P5C solution just before the assay and avoid acidification of the assay mixture.

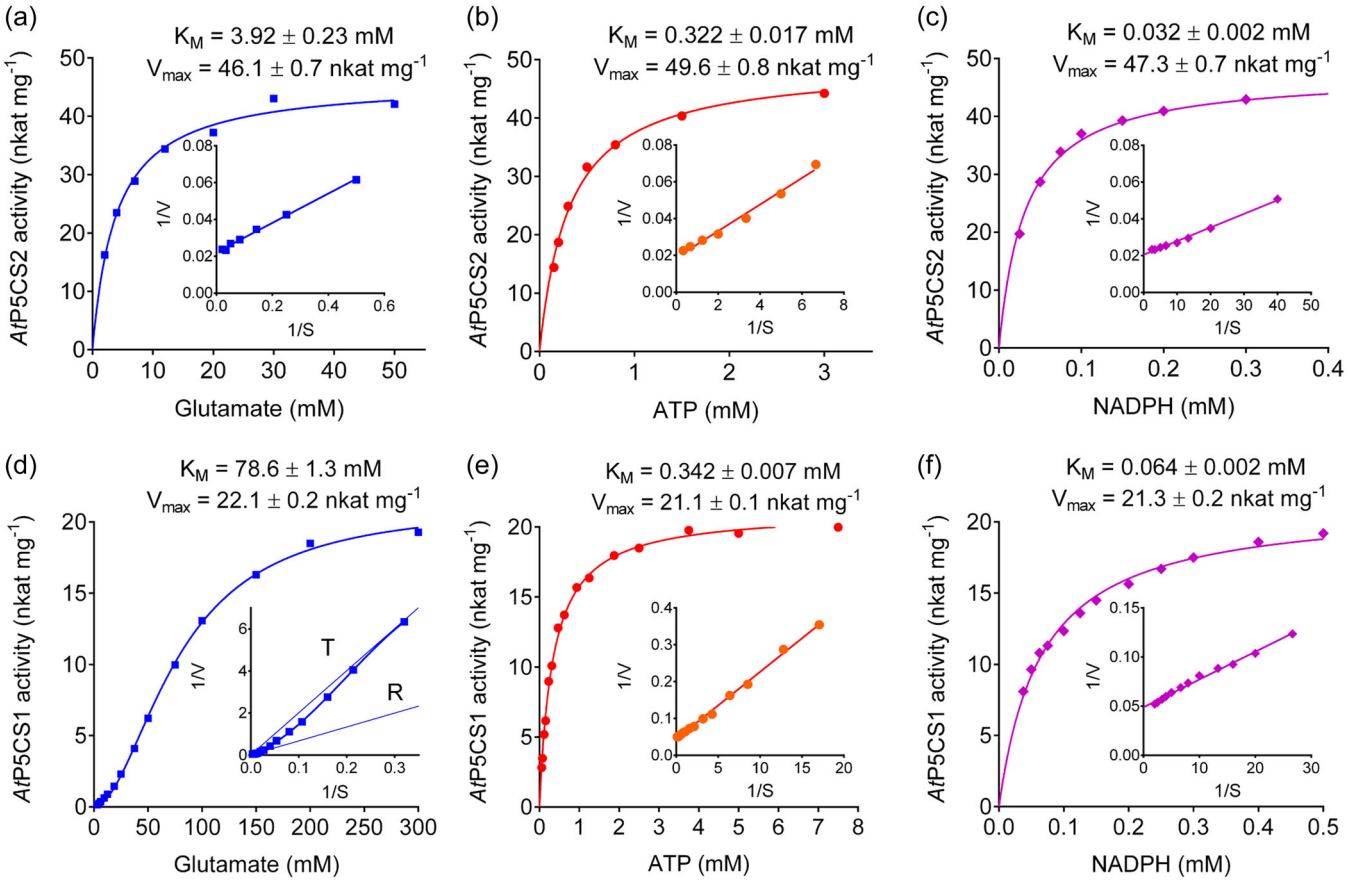

FIGURE 2 Substrate-activity relationships for *Arabidopsis thaliana* P5CS isoenzymes. The purified enzymes were assayed in the presence of increasing concentrations of glutamate (a) and (d) for *At*P5CS2 and *At*P5CS1, respectively, ATP (b) and (e) or NADPH (c) and (f) while maintaining those of the other two substrates at near saturating levels, as detailed in Section 2. Lineweaver–Burk plots of the data (Insets) allowed the calculation of V_{MAX} and K_M values, estimated by using the corresponding functions in Prism 6 for Windows, version 6.03. In the case of *At*P5CS1, for which a sigmoidal curve was obtained suggesting positive cooperativity with respect to glutamate, the equation $Y = V_{MAX} \times X^h / (K_{half}{}^h K_M{}^h + X^h)$ was used instead to estimate the K_M value (K_{half}) and the Hill-coefficient (h). Data in Lineweaver–Burk plot – inset of (d) – show the progressive transition from the *T* state (low affinity) to the *R* state (high affinity), as the saturation increases. [Color figure can be viewed at wileyonlinelibrary.com]

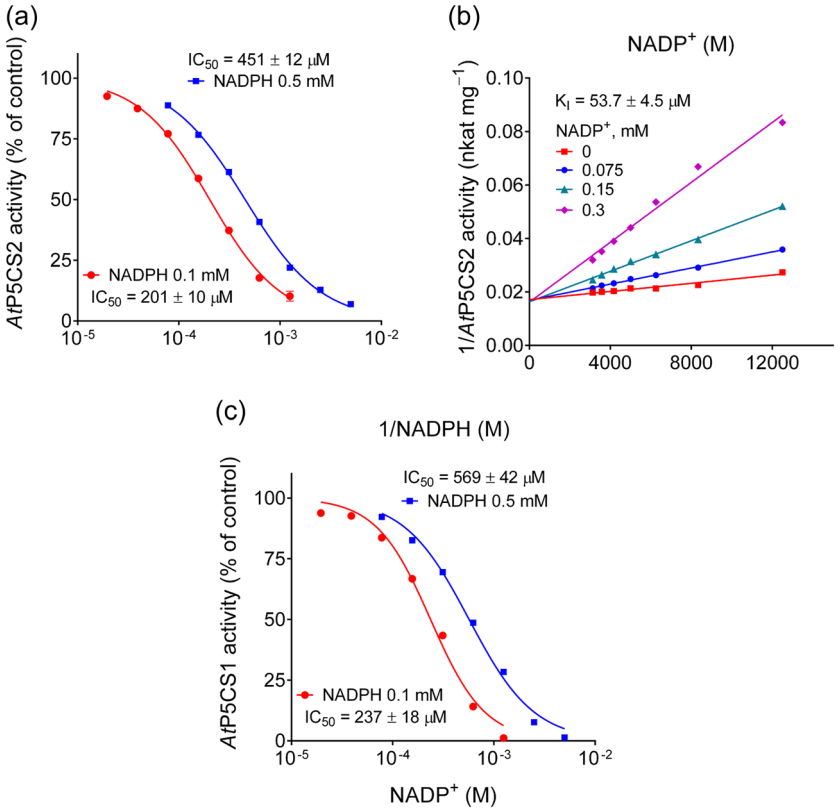

FIGURE 3 Effect of $NADP^+$ on the activity of *Arabidopsis thaliana* P5CS isoenzymes. *At*P5CS2 and *At*P5CS1 were assayed in the presence of increasing concentrations of $NADP^+$, and the resulting activity was plotted as percent of that obtained in its absence (a) and (c), respectively. Nonlinear regression of data allowed calculation of the respective concentrations inhibiting activity by 50% (IC_{50}). Since a reduction of NADPH in the reaction mixture was found to increase the inhibitory effect of $NADP^+$, the substrate-activity relationship of *At*P5CS2 was assessed in the presence of increasing levels of the product. Lineweaver–Burk plots of data showing lines converging on the *y*-axis accounted for an inhibition of competitive type. The calculated K_I value is also shown (b). [Color figure can be viewed at wileyonlinelibrary.com]

3.3 | The activity of *At*P5CS2 is feedback inhibited by proline, and inhibited by arginine, ornithine and glutamine, but the resulting effect depends on glutamate concentration

P5CS2 is believed to regulate the carbon flux to produce the amount of proline required for protein synthesis and is therefore expected to be feedback inhibited by the final product. When the activity of the purified *At*P5CS2 was assayed in the presence of increasing concentrations of proline, a dose-dependent inhibition was indeed evident (Figure 6a). However, from a quantitative point of view, the effect was milder than expected, with an IC_{50} value of 77 mM that is 10- to 20-fold higher than those reported for the enzyme from *Vigna aconitifolia* (Zhang et al., 1995) and rice (Sabbioni et al., 2021). However, when the concentration of glutamate in the reaction mixture was lowered from saturating levels to a concentration near to the K_M value, an IC_{50} (10 mM) of the same order of magnitude than those reported in previous studies was obtained. A thorough kinetic analysis showed that proline inhibits the enzyme with a mechanism of competitive type with respect to both glutamate and ATP (Figure 6b,c) and of uncompetitive type with respect to NADPH (Figure 6d). The calculated K_I values were 4, 4 and 47 mM for glutamate, ATP and NADPH, respectively. If the corresponding K_I/K_M ratio is considered, while those for ATP and NADPH suggested a low binding affinity (13.9 and 1466, respectively), that for glutamate was close to the unit (1.04), supporting a relatively high affinity of the inhibitor to the active site of the enzyme.

The possibility that other, metabolically related compounds could inhibit enzyme activity was also considered. When added to the standard assay mixture, glutamine, arginine and ornithine reduced the catalytic rate only at levels exceeding 100 mM. If the concentration of glutamate was reduced to near the K_M value, both glutamine and arginine were found to progressively inhibit enzyme activity in the 10–100 mM range (Figure 7a,c), with IC_{50} values of 77 and 148 mM, respectively. The kinetic analysis confirmed the competitive type of the inhibition with respect to glutamate (Figure 7b,d), with K_I values of 28 mM for glutamine and 71 mM for arginine. Ornithine was less effective, with an IC_{50} value of 228 mM (Figure 7e).

3.4 | *At*P5CS1 shows the same absolute requirement for Mg^{2+} ions, but it is less influenced by the presence of monovalent cations

The heterologous expression of the other, stress-induced P5CS isoenzyme was obtained more easily, although even in this case a significant amount of the protein produced in *E. coli* was sequestered in inclusion bodies. To limit this drawback, once again the induction by IPTG was carried out at low temperature and for a long time. The heterologous protein was expressed at lower levels than *At*P5CS2, as judged by the less pronounced band obtained by SDS-PAGE analysis of total extracts (Supporting Information S1: Figure S4). Conversely, affinity chromatography of the His-tagged protein yielded greater

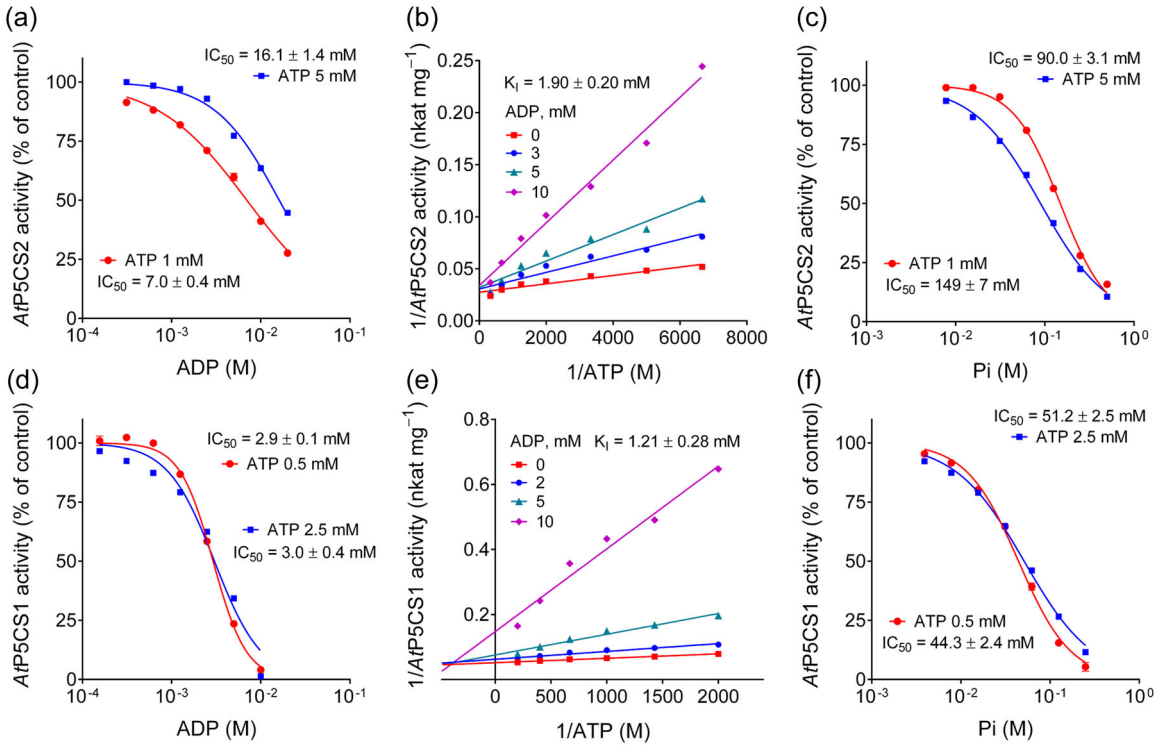

FIGURE 4 Effect of ADP and inorganic phosphate (Pi) on the activity of *Arabidopsis thaliana* P5CS isoenzymes. The two isoenzymes were assayed in the presence of increasing concentrations of ADP or Pi, and the resulting activity was plotted as percent of that obtained in their absence (a) and (c) for *At*P5CS2, and (d) and (f) for *At*P5CS1, respectively. Nonlinear regression of data allowed calculation of the concentrations inhibiting activity by 50% (IC_{50}). Since a reduction of ATP in the reaction mixture was found to increase the inhibitory effect of ADP, the substrate-activity relationship was assessed in the presence of increasing levels of the product. In the case of *At*P5CS2, Lineweaver–Burk plots of data showing lines converging on the *y*-axis accounted for an inhibition of competitive type (b). For *At*P5CS1, Lineweaver–Burk plot of data showing lines that intersect in the second quadrant suggested on the contrary an inhibition of mixed type (e). The calculated K_I values are also indicated. [Color figure can be viewed at wileyonlinelibrary.com]

amounts of the enzyme, yet its high instability required daily preparations to be used for the biochemical characterization.

The addition of Mg^{2+} ions to the reaction mixture stimulated tenfold the low basal activity, which was completely abolished in the presence of 1 mM EDTA, confirming, also in this case, an absolute requirement for Mg^{2+}. Maximal activity was obtained at 1–10 mM Mg^{2+}, whereas concentrations exceeding this threshold were found inhibitory (Figure 1d). Ca^{2+} up to 10 mM did not revert the stimulatory effect of Mg^{2+}. The addition of K^+ and NH_4^+ in the 10^{-3} to 10^{-1} M range only slightly increased enzyme activity, while Na^+ was completely ineffective (Figure 1e). Above 100 mM, anions steadily inhibited the activity of *At*P5CS1 (Figure 1f).

3.5 | *At*P5CS1 has a very high K_M value for glutamate with characteristics of cooperative substrate binding and is stimulated by P5C in the presence of low glutamate concentrations

The specific activity level of purified *At*P5CS1 under standard assay conditions was lower than that of *At*P5CS2, being equal to 19.6 ± 0.5 nkat mg^{-1} (n = 28). Even at near saturating conditions the estimated V_{MAX} (22 nkat mg^{-1} protein) corresponded to a catalytic constant of about 2 s^{-1}. Interestingly, maximal activity required a very high concentration of glutamate. Kinetic analysis showed that, while the K_M values for ATP and NADPH were similar to those calculated for *At*P5CS2 (Figure 2e,f), *At*P5CS1 showed a 20-fold higher K_M value for glutamate (79 vs. 4 mM). Moreover, the stress-induced isoenzyme displayed a sigmoidal kinetic response to increasing glutamate concentrations (Figure 2d) that is characteristic of positive cooperativity. The calculated Hill slope (1.9–2.9) suggested the presence of several interacting binding sites.

When the possible occurrence of product inhibition was considered, $NADP^+$ was found to interfere with the activity of *At*P5CS1 with the same characteristics previously shown for *At*P5CS2 and with a similar quantitative effect (Figure 3c). Conversely, the inhibition brought about by ADP was different. The IC_{50} value did not change at varying the concentration of ATP in the reaction mixture (Figure 4d), and a kinetic analysis showed a decreased V_{MAX} in the presence of increasing inhibitor levels. The Lineweaver–Burk plot of the data was consistent with an inhibition mechanism of mixed type (Figure 4e), suggesting that in this case, the inhibitor may bind the enzyme either if complexed or not with ATP. However, a high α value (7.48) accounted for a higher affinity to the enzyme that has not already bound the substrate. Inorganic phosphate

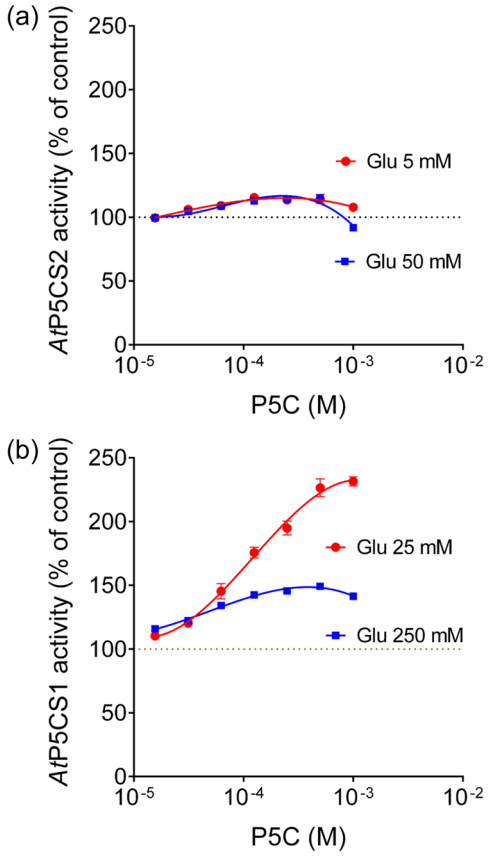

FIGURE 5 Effect of P5C on the activity of *Arabidopsis thaliana* P5CS isoenzymes. *At*P5CS2 and *At*P5CS1 were assayed in the presence of increasing concentrations of P5C, and the resulting activity was plotted as percent of that obtained in its absence (a) and (b), respectively. Enzyme activity was measured either at saturating glutamate concentrations or in the presence of tenfold lower levels of the substrate. P5C, δ^1-pyrroline-5-carboxylate. [Color figure can be viewed at wileyonlinelibrary.com]

was found to inhibit *At*P5CS1 only at high levels (IC_{50} value of about 50 mM; Figure 4f). Interestingly, when the effect of increasing concentrations of P5C was investigated, a different effect was found in the presence of various levels of glutamate. Under near saturating conditions, a slight stimulation was evident, similar to that previously found for *At*P5CS2. On the contrary, in the presence of a limiting substrate concentration, a more marked stimulation by P5C was evident in the 10^{-4} to 10^{-3} M range (Figure 5b). With the carry-over of ions being the same in the two cases, this suggests a specific effect of P5C.

3.6 | *At*P5CS1 activity showed weak sensitivity to feedback inhibition by proline, and in the presence of low glutamate levels was strongly stimulated by glutamine

Being the isoenzyme responsible for the synthesis of proline to be accumulated under stress, *At*P5CS1 was expected to be almost insensitive to feedback inhibition. In fact, when increasing levels of proline were added to the assay mixture, enzyme inhibition took place only at over 100 mM. At saturating substrate concentrations, the calculated IC_{50} value for proline was threefold higher than that of *At*P5CS2 (224 vs. 77 mM). However, when the experiment was repeated in the presence of a limiting concentration of glutamate, the apparent sensitivity of *At*P5CS1 did not increase. In the 10–100 mM proline range, enzyme activity was on the contrary slightly stimulated (Figure 6e), and at higher concentrations, the inhibitory effect was proportional to the concentration of the substrate (not shown). When the substrate-activity relationship for glutamate was evaluated in the presence of the final product of the pathway, the higher the concentration of proline, the more the obtained curve approached a canonical hyperbolic pattern (Figure 6f). Consistently, the Hill coefficient progressively decreased and came close to one (Figure 6g), suggesting that the binding of proline could *mimic* that of glutamate and facilitate the binding of the substrate to another subunit. With respect to the other two substrates, an inhibition mechanism of competitive type against ATP (Figure 6h) and uncompetitive toward NADPH (Figure 6i) was found also for *At*P5CS1, but with K_I values 10- to 20-fold higher than those found for *At*P5CS2.

When a possible inhibitory effect of related amino acids was assessed, a very similar pattern as for *At*P5CS2 was found in the case of arginine (Figure 7f) and ornithine (not shown). On the contrary, a completely different result was evident for glutamine. In the presence of saturating glutamate concentrations, glutamine was ineffective up to 125 mM. However, when the enzyme was incubated with limiting glutamate levels, the addition of increasing concentrations of glutamine was found to strongly promote *At*P5CS1 activity, with a fourfold stimulation at the maximal dose tested (Figure 7g). In this case also, when the substrate-activity relationship for glutamate was evaluated in the presence of increasing levels of glutamine, the higher the concentration of the latter, the more the obtained curve shifted from a sigmoidal to a hyperbolic pattern (Figure 7h,i). This suggests that, similarly to proline, the binding of glutamine could simulate that of the substrate and facilitate the binding of glutamate to another subunit.

4 | DISCUSSION

To the best of our knowledge, this is the first report to compare the properties of a P5CS isozyme pair in a higher plant. Both recombinant *A. thaliana* P5CS isoenzymes tended to form aggregates in *E. coli* and showed low stability after purification, with less than 20% of residual activity remaining after 24 h storage at 4°C. Removal of the N-terminal His-tag from *At*P5CS1 did improve neither specific activity levels nor enzyme stability. On the contrary, a significant loss of activity occurred during incubation with TEV protease and the subsequent negative chromatography, needed to remove the His-tag used for purification. Therefore, enzyme characterization was performed with the His-tagged proteins. The theoretical possibility exists that the presence of the His-tag may somehow affect *At*P5CS

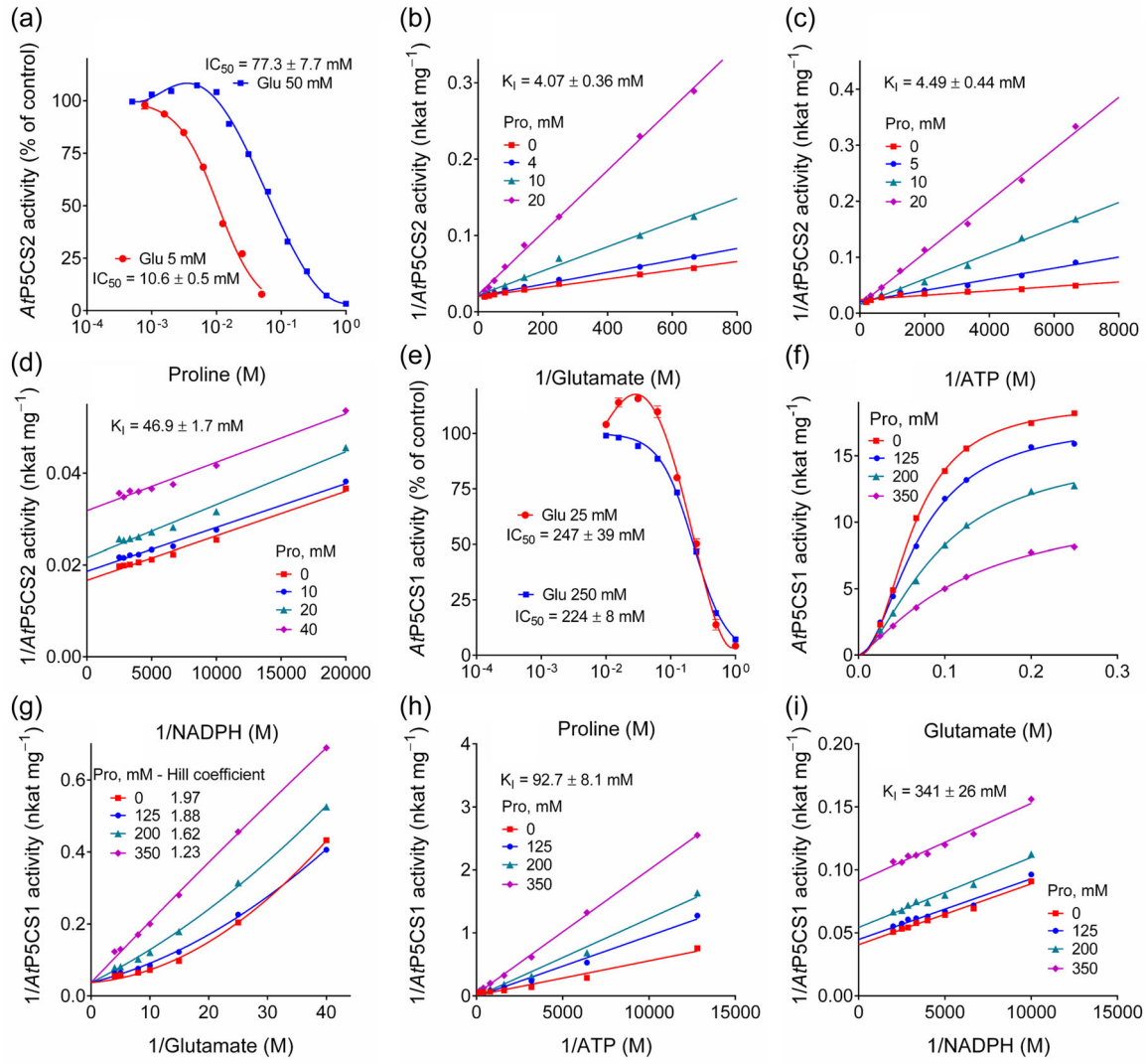

FIGURE 6 Effect of proline on the activity of *Arabidopsis thaliana* P5CS isoenzymes. The activity of either isoenzyme was measured under standard assay conditions in the presence of increasing concentrations of proline, and the results were plotted as percent of those in the absence of proline (a) and (e) for *At*P5CS2 and *At*P5CS1, respectively. Nonlinear regression of the data allowed calculation of the concentration inhibiting activity by 50% (IC_{50}), which was found to be reduced when the assay was repeated in the presence of a limiting concentration of glutamate. In the case of *At*P5CS2, when the substrate-activity relationship was assessed for glutamate (b), ATP (c) and NADPH (d) in the presence of increasing proline levels, the Lineweaver–Burk plot of the data showed lines intersecting on the *y*-axis for glutamate and ATP, and parallel lines in the case of NADPH, suggesting a competitive and an uncompetitive inhibition type, respectively. The corresponding K_I values are indicated. In the case of *At*P5CS1, when the substrate-activity relationship for glutamate was assessed in the presence of increasing proline levels (f), the obtained curves shifted from a sigmoidal to a hyperbolic pattern. Accordingly, the Lineweaver–Burk data transformation showed a straight line only in the presence of high proline concentrations (g). In the case of ATP and NADPH, the double reciprocal plots obtained in the absence or in the presence of proline confirmed an inhibition of competitive and uncompetitive type (h) and (I), respectively, although higher K_I values were found. [Color figure can be viewed at wileyonlinelibrary.com]

activity. However, this possibility has been proven in a very limited number of cases, if any. Moreover, both the N- and the C-terminus, where the His-tag of *At*P5CS1 and *At*P5CS2 were located, respectively, protrude from otherwise compact domains in the predicted three-dimensional structure of the enzyme (Supporting Information S1: Figure S5), making it unlikely that the tag altered enzyme properties.

The two *A. thaliana* isoenzymes showed an absolute requirement of Mg^{2+} ions for activity, a feature that is not shared by P5CS2 from rice (Sabbioni et al., 2021). This inconsistency might reflect a somehow different catalytic mechanism or depend on a different ability of the enzyme to retain bound Mg^{2+} during extraction and purification. Similar to the *At*P5CS isoenzymes, the activity of GK from *E. coli* (ProB) was dependent on Mg^{2+} (Pérez-Arellano et al., 2005). This dependency was reduced when the C-terminal pseudouridine synthase and archaeosine transglycosylase domain was deleted, which is believed to be involved in oligomerization or mediating the interaction with GPR in prokaryotes and fungi. The

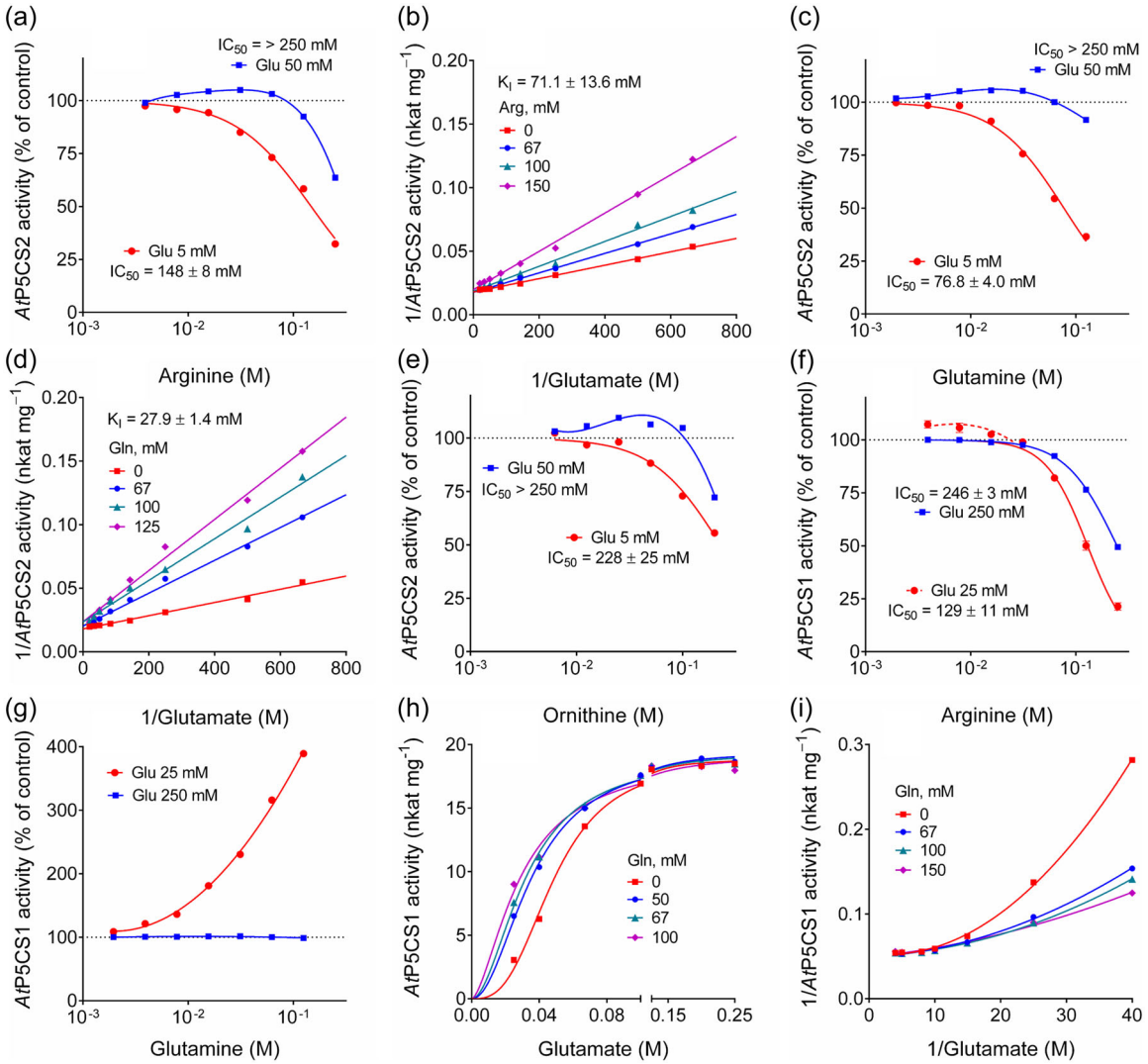

FIGURE 7 Effect of metabolically related amino acids on the activity of *Arabidopsis thaliana* P5CS isoenzymes. *At*P5CS2 was incubated in the presence of increasing concentrations of arginine (a), glutamine (c) or ornithine (e), in a reaction mixture containing either limiting or nonlimiting levels of glutamate. After plotting data as percent of the values obtained in the absence of any addition, the corresponding concentrations inhibiting activity by 50% (IC_{50}) were calculated by nonlinear regression of data. When the affinity toward glutamate was determined in the presence of increasing levels of arginine (b) or glutamine (d), lines converging on the *y*-axis in Lineweaver–Burk plots suggested in both cases a mechanism of competitive type and allowed calculations of K_I values. When *At*P5CS1 was incubated in the presence of increasing concentrations of arginine (f) or glutamine (g), similar IC_{50} values were obtained for arginine. On the contrary, the addition of glutamine in the presence of limiting concentrations of the substrate caused activity stimulation. Therefore, the affinity toward glutamate was determined in the presence of increasing levels of glutamine (h). Lineweaver–Burk transformation of data showed that only in the presence of high glutamine levels the double reciprocal plot approached a *canonical* straight line (i). [Color figure can be viewed at wileyonlinelibrary.com]

Mg^{2+} ions might be needed for oligomer formation or to compensate the negative charges of the phosphate groups of ATP. In support of the latter hypothesis, a Mg^{2+} ion was found between ADP and γ-glutamylphosphate in the cryo-EM structure of the GK domain of *Drosophila melanogaster* P5CS (PBB 7WX3; Zhong et al., 2022).

*At*P5CS2 showed also a lower sensitivity to proline and a higher stimulation by cations than *Os*P5CS2. It needs to be emphasized that in the case of P5CS, it is expected that the isoforms in different species have distinct properties, because P5CS duplication occurred several times following the emergence of flowering plants and at different frequencies throughout the evolution of monocots and dicots (Supporting Information S1: Figure S2) (Turchetto-Zolet et al., 2009). In contrast other isoenzyme pairs, such as those of several enzymes in the shikimate pathway, displayed higher similarity with orthologues from other species than within one species (Forlani et al., 2023). Therefore, a substantial variability could exist with respect to P5CS functional properties both between the two paralogs of the same plant and among homologs of different species. This seems true also at the transcriptional level, with the isogenes from *A. thaliana* showing a more definite divergent evolution of role and regulation than the rice counterparts: under osmotic stress conditions, proline accumulation in *A. thaliana* seems to depend almost exclusively on

transcriptional *AtP5CS1* induction (Funck et al., 2020), whereas in rice both *OsP5CS* genes are activated (Forlani, Bertazzini, Zarattini, & Funck, 2015).

The apparent K_M values for glutamate, ATP and NADPH found for *At*P5CS2 are similar to those previously shown for the rice homolog (Sabbioni et al., 2021), while a noteworthy difference was evident with respect to the sensitivity to proline (a 26-fold higher IC_{50} value at saturating levels of substrates). If the intracellular level of free proline was being determined only by feedback inhibition of P5CS, a remarkable dissimilarity would be expected in the two species. On the contrary, similar proline concentrations were found in cultured cells of *A. thaliana* (0.18 μmol g^{-1} FW [Forlani et al., 2013] and rice [0.20–0.65 μmol g^{-1} FW; Forlani et al., 2014; Forlani, Bertazzini, Zarattini, & Funck, 2015]). Because proline inhibits *At*P5CS2 with a mechanism of competitive type with respect to glutamate and ATP, the extent of feedback inhibition is influenced by the actual concentration of the substrates, mainly by glutamate, whose K_M value (3.9 mM) is very close to the corresponding K_I value for proline (4.1 mM). As glutamate occupies a major portion of the free amino acid pool, its amount was found relatively constant under various conditions in the same plant (Ishizaki et al., 2010) and seems not dissimilar in *A. thaliana* (0.79 μmol g^{-1} FW; Forlani et al., 2013) and rice (0.4–0.6 μmol g^{-1} FW; Forlani et al., 2014). These results thus suggest that the homoeostatic level of proline depends more on glutamate availability than on feedback inhibition of *At*P5CS2. If the above data were converted into molar levels on the assumption of an intracellular volume equal to about 30%–40% of the total water content in Arabidopsis cultured cells, a glutamate concentration is obtained (2–3 mM) that is indeed very close to the K_M value. This would also imply that a strict dependence may exist between the intracellular level of proline and that of glutamate. Consistently, induced variations in glutamate levels were found to impact upon both proline homoeostasis (Brugière et al., 1999) and its accumulation under stress (Díaz et al., 2010).

A similar conclusion may be drawn also for NADPH. Both *A. thaliana* P5CS isoenzymes were found to be inhibited by $NADP^+$, with a K_I value (about 50 μM) that is very close to the K_M values for NADPH (32 and 64 μM for *At*P5CS2 and *At*P5CS1, respectively). $NADP^+$ and NADPH levels in *A. thaliana* seedlings usually range from 2 to 25 and 1 to 2 nmol g^{-1} FW, respectively (Queval & Noctor, 2007; Sharma et al., 2011; Takahashi et al., 2009), values that can be approximatively converted to 100–1250 and 50–100 μM, respectively. The flux toward proline biosynthesis may therefore be constitutively limited by both low NADPH availability and inhibitory $NADP^+$ levels. This implies that any change in the NADPH/$NADP^+$ ratio may greatly influence P5CS activity, and in turn the homoeostatic level of proline, by a simple overflow effect. Changes in other physiological functions that cause a variation in the NADPH/$NADP^+$ ratio are frequently linked with altered proline production and vice versa (Alvarez et al., 2022; Hare & Cress, 1997). The response of P5CS activity to the NADPH/$NADP^+$ ratio can represent the long-awaited molecular basis for these effects. *A. thaliana* plants over-expressing NAD kinase 2, for example, showed increased levels of free proline (Takahashi et al., 2009). Arabidopsis mutants partially defective in either proline synthesis or catabolism showed a more reduced NADPH/$NADP^+$ ratio at low water potential (Sharma et al., 2011). Mutants impaired in very long-chain fatty acid synthesis showed an altered cellular redox status, which correlated with increased proline accumulation at low water potential. Consistently, the NADPH oxidase inhibitor diphenyleneiodonium induced high levels of proline accumulation (Shinde et al., 2016). A rice knockout mutant for NAD kinase 1 had a decreased NADP(H)/NAD(H) ratio and exhibited increased sensitivity to drought. The over-expressing plants showed a dramatic increase in free proline content (Wang et al., 2020). Transgenic *Nicotiana tabacum* plants with glucose-6-phosphate dehydrogenase isoenzyme replacement in the cytosol were found to maintain a higher NADPH/$NADP^+$ ratio under light and to accumulate higher proline levels under salt stress (Scharte et al., 2023). All these results strengthen the probability that the availability of NADPH is a main constraint limiting proline biosynthesis. This also implies that P5CS activity can function as a mechanism to prevent over-reduction of the NADP(H) pool without the need for transcriptional adjustment. On the contrary, the possibility that P5CS inhibition by ADP can play a significant role in vivo seems less likely. The K_I values found (1–2 mM) were three- to sixfold higher than the K_M values for ATP, and in *A. thaliana* seedlings, the ATP/ADP ratio has been shown to vary between 2 and 3 (Liang et al., 2015). Moreover, the absolute ATP content (20–25 nmol g^{-1} FW) should correspond to 500–600 μM, about twice the concentration ensuring 50% of maximal enzyme activity. This notwithstanding, it cannot be ruled out that under some circumstances a lowering in either the absolute concentration of ATP or the ATP/ADP ratio may also limit proline biosynthesis.

The biochemical characterization of *At*P5CS2 also confirmed previous data obtained with the rice homolog showing enzyme inhibition by arginine, ornithine and glutamine, which are metabolically related to proline and glutamate (Supporting Information S1: Figures S1 and S6). This could support the early hypothesis that the glutamate pathway is the main route for proline synthesis in plants only under nitrogen limitation, whereas under high nitrogen input, resulting in high glutamine and arginine levels, the ornithine pathway assumes prominence (Delauney & Verma, 1993). However, the occurrence of the ornithine pathway has been excluded in *A. thaliana* (Funck et al., 2008), and the sensitivity of *At*P5CS2 seems too low to provide the molecular basis of such regulative mechanism. This notwithstanding, it cannot be ruled out that in some cells arginine and glutamine may be accumulated as nitrogen storage compounds and reach levels high enough to effectively inhibit *At*P5CS2 activity. On the other hand, all plant P5CS sequences lack the residues that were found to mediate the inhibition of human P5CS by ornithine (Supporting Information S1: Figure S2; Hu et al., 1999), and it is therefore unclear why *Os*P5CS2 and the isoenzymes from *A. thaliana* differ in this respect.

Noteworthy is, on the other hand, the finding that *At*P5CS2 activity is progressively stimulated by K^+ cations in the 1–100 mM range. K^+ accumulation is a widespread strategy in plants to

counteract the negative effects of excess salt in the soil (Bertazzini et al., 2018). Therefore, K^+-mediated stimulation of *At*P5CS2 activity could ensure a prompt and significant increase of proline synthesis upon the exposure to salt stress conditions even before transcriptional *At*P5CS1 induction. This mechanism could ensure immediate protection of meristematic cells, where expression of *At*P5CS2 is the highest and where – according to the poor growth of *p5cs2* mutants – the activity of *At*P5CS1 is insufficient (Funck et al., 2012; Székely et al., 2008).

Anyway, it is well established that stress-induced proline accumulation in *A. thaliana* is driven mainly by the upregulation of *At*P5CS1 expression (Funck et al., 2020). The functional features of this second isoenzyme strengthen this conclusion. Despite both isoenzymes having the Asp_{125} and Phe_{128} residues (Supporting Information S1: Figure S2) that have been identified as critical amino acids for the mechanism of feedback inhibition by proline (Zhang et al., 1995), *At*PCS1 showed a reduced sensitivity to proline that may favour the accumulation of proline to high concentrations. Instead of Thr_{124}, which is highly conserved among plant P5CS sequences including *At*P5CS2, *At*P5CS1 has an Asn residue that could affect the binding of proline. This residue was not analyzed in the study establishing the importance of Phe_{128} in feedback inhibition (Zhang et al., 1995), and we are not aware of reports about modifications in this position in any other species. In bacterial and fungal GK enzymes, residues involved in feedback inhibition by proline cluster at and around the binding site for glutamate (Supporting Information S1: Figure S2; Pérez-Arellano et al., 2005; Pérez-Arellano et al., 2006, 2010; Sekine et al., 2007). For most of the differences between *At*P5CS1 and *At*P5CS2 at or around the putative glutamate binding site, *At*P5CS1 is closer to the plant P5CS consensus sequence, making Thr_{124} the best candidate to explain the virtual absence of feedback inhibition in *At*P5CS1. In an overlay of the modelled *At*P5CS2 structure with the cryo-EM structure of *D. melanogaster* P5CS (Supporting Information S1: Figure S5; Zhong et al., 2022), Asp_{125} and Phe_{128} of *At*P5CS2 are more than 11 Å away from glutamate. This suggests that either the model is incorrect or the mechanism of feedback inhibition by proline differs strongly between the GK domain of plant P5CS and bacterial and fungal GK enzymes. Further structural or mutational studies will be required to determine the mechanism of proline inhibition of plant P5CS enzymes and to explain the differences between *At*P5CS2 and *At*P5CS1 in this respect.

The presence of increasing levels of proline was even found to stimulate enzyme activity when the concentration of glutamate was limiting. The kinetic analysis of the purified protein revealed that *At*P5CS1 is a hysteretic enzyme that shows positive cooperativity at increasing substrate concentrations. This feature seems to compensate other properties that would apparently disfavour the synthesis of proline under stress. In fact, *At*P5CS1 showed a low V_{MAX}, corresponding to only 2 catalytic events s^{-1}, and a high K_M for glutamate of about 80 mM. These data once again suggest that the rate of P5C synthesis is responsive to the concentration of glutamate. Yet, from a quantitative point of view, the disclosed cooperative mechanism would imply that no substantial amounts of P5C may be produced by *At*P5CS1 in the presence of the glutamate levels that have been measured in *A. thaliana* cultured cells and seedlings (see above). However, our data showed that the dose–response of the enzyme to the glutamate level is greatly influenced by other factors, namely, the concentrations of proline, P5C and – most interestingly – glutamine. The presence of increasing levels of these compounds were found to shift the dose–response curve to glutamate from a sigmoidal to a hyperbolic pattern, suggesting that their binding to the enzyme facilitates substrate binding in other enzyme subunit(s), and allows significant activity even in the presence of physiological, low levels of glutamate. The stimulatory effect exerted by proline may facilitate the attainment of a homoeostatic level at a higher concentration. The effect of P5C most likely does not have any relevance in vivo, since the levels of this, possibly toxic, intermediate (Deuschle et al., 2004; Qamar, Mysore, & Senthil-Kumar, 2015) are maintained very low in the cell (Giberti et al., 2017; Monteoliva et al., 2014). Moreover, the specific activity of plant P5C reductase is thousand-fold higher (Forlani, Bertazzini, Zarattini, Funck, Ruszkowski, et al., 2015; Giberti et al., 2014) than that found in this and other works (Sabbioni et al., 2021) for P5CS, suggesting that P5C is promptly reduced to proline as soon as it is produced. The effect of glutamine may provide a mechanism to allow a quantitative synthesis of proline only in the presence of a nonlimiting amount of organic nitrogen. Contrary to glutamate, which is maintained at a relatively constant level in the plant cell (Ishizaki et al., 2010), glutamine is used in several species as a nitrogen storage compound (Nordin & Näsholm, 1997), and its concentration may vary significantly. Indeed, the glutamine level (or the glutamine-to-glutamate ratio) is believed to be an index of nitrogen availability and may be used by the plant cell to sense its nitrogen status and regulate selected aspects of nitrogen metabolism (Chellamuthu et al., 2014; Forlani et al., 2023; Gent & Forde, 2017). The stimulatory effect of glutamine on *At*P5CS1 activity in the presence of low concentrations of glutamate may thus represent a control switch to avoid nitrogen depletion deriving from sustained proline synthesis in the absence of sufficient nitrogen supply.

The results obtained so far do not permit us to depict the molecular mechanism underlying enzyme cooperativity. Several attempts to characterize the composition of the *At*P5CS1 holomer by either native polyacrylamide gel electrophoresis or gel permeation chromatography failed. In *D. melanogaster*, it has recently been reported that P5CS forms filaments in vivo (Zhang et al., 2020). The use of cryo-electron microscopy showed that divergent helical filaments were assembled from P5CS tetramers and stabilized by multiple interfaces. Point mutations disturbing those interfaces prevented *Dm*P5CS filament formation and greatly reduced the enzymatic activity (Zhong et al., 2022). Interestingly, glutamate was found to promote the formation and maintenance of Drosophila P5CS filaments (Zhang et al., 2020). Multimerization of *Dm*P5CS was found to be altered by stress conditions and led to hypothesize that this may represent a sensing mechanism to perceive cellular stress and modulate metabolism by regulating mitochondrial respiration (Yang et al., 2021). The plant system is most likely different, in that P5CS has a different subcellular localization (cytosolic and not mitochondrial), and stress conditions

should promote and not reduce P5CS activity. The oligomerization domains that mediate tetramer formation in *Dm*P5CS are well conserved among P5CS sequences from animals and plants (Supporting Information S1: Figure S2; Zhong et al., 2022). In contrast, the amino acids identified to mediate filament formation in *Dm*P5CS are not conserved in plant P5CS enzymes, but according to AlphaFold structure predictions, the enzymes may assume a very similar monomer structure (Supporting Information S1: Figure S5). Moreover, large fluorescent structures were observed in plants expressing *At*P5CS1:GFP fusion proteins (Székely et al., 2008). It remains to be determined if this reflects functional higher-order oligomers, and if oligomer formation promotes or inhibits the activity of plant P5CS enzymes. Despite the differential localization, both human and *A. thaliana* P5CS are reported to be phosphorylated (Ser_{78} and Ser_{79} in *At*P5CS1 and 2 and Ser_{136} and others in *Hs*P5CS1; PhosPhAT and UniProt databases). These Ser residues are within a region corresponding to the interface of *Dm*P5CS that mediates filament formation (Supporting Information S1: Figure S2), but the functional consequences of their phosphorylation are presently unknown. However, a mechanism of enzyme activation by multimerization, regulated by phosphorylation and stimulated by glutamate, proline and glutamine binding, might explain several of the results obtained in this study. Furthermore, oligomerization-dependent activation of constitutively expressed *At*P5CS1 might allow a more rapid response to stress conditions than transcriptional upregulation. At the same time, a low activity of *At*P5CS1 in unstressed cells may be desired to avoid wasting of ATP and NADPH in mature tissues, where the demand for proline for protein synthesis is low. In unstressed cells, high proline levels would activate proline degradation by induction of ProDH expression and thus create a futile cycle (Trovato et al., 2019). Several polymorphisms between *At*P5CS1 and *At*P5CS2 cluster in a region of the GPR catalytic domain that is required for higher-order oligomer formation in *Dm*P5CS (Supporting Information S1: Figure S2). A greater capacity of *At*P5CS1 for oligomerization-dependent activation may be a reason why this isoform is especially important for stress-induced proline accumulation (Funck et al., 2020; Sharma et al., 2011; Székely et al., 2008). Determination of the three-dimensional structure of the plant P5CS enzyme will allow to confirm or reject such hypotheses.

Together with further mechanistic and structural studies, the present set of information may contribute to a better understanding of the regulation and functional relevance of proline biosynthesis in plants. Different functions can be expected under either normo-osmotic or stress conditions, satisfying the needs of protein biosynthesis, osmoprotection and redox regulation. If confirmed with P5CS enzymes from other plant species, our results can provide new perspectives for metabolic engineering and hopefully facilitate the future attainment of plant varieties with increased tolerance to water and salt stress.

ACKNOWLEDGEMENTS

This work was supported by grants from the University of Ferrara to Giuseppe Forlani (*Fondo di Ateneo per la Ricerca* 2020, 2021 and 2022). Giuseppe Sabbioni was recipient of a PhD scholarship from the Italian Ministry of University and Research. Simone Barera acknowledges support from the National Recovery and Resilience Plan (NRRP), Mission 04 Component 2 Investment 1.5 – NextGenerationEU, Call for tender n. 3277 dated 30 December 2021, award number 0001052 dated 23 June 2022.

DATA AVAILABILITY STATEMENT

The data that support the findings of this study are available from the corresponding author upon reasonable request.

ORCID

Giuseppe Forlani http://orcid.org/0000-0003-2598-5718
Giuseppe Sabbioni http://orcid.org/0000-0002-3251-7712
Simone Barera http://orcid.org/0000-0001-6009-1205
Dietmar Funck http://orcid.org/0000-0002-9855-0419

REFERENCES

Alvarez, M.E., Savouré, A. & Szabados, L. (2022) Proline metabolism as regulatory hub. *Trends in Plant Science*, 27(1), 39–55. Available from: https://doi.org/10.1016/j.tplants.2021.07.009

Bertazzini, M., Sacchi, G.A. & Forlani, G. (2018) A differential tolerance to mild salt stress conditions among six Italian rice genotypes does not rely on Na^+ exclusion from shoots. *Journal of Plant Physiology*, 226, 145–153. Available from: https://doi.org/10.1016/j.jplph.2018.04.011

Bradford, M.M. (1976) A rapid and sensitive method for the quantitation of microgram quantities of protein utilizing the principle of protein-dye binding. *Analytical Biochemistry*, 72, 248–254. Available from: https://doi.org/10.1006/abio.1976.9999

Brugière, N., Dubois, F., Limami, A.M., Lelandais, M., Roux, Y., Sangwan, R.S. et al. (1999) Glutamine synthetase in the phloem plays a major role in controlling proline production. *The Plant Cell*, 11(10), 1995–2011. Available from: https://doi.org/10.1105/tpc.11.10.1995

Chellamuthu, V.R., Ermilova, E., Lapina, T., Lüddecke, J., Minaeva, E., Herrmann, C. et al. (2014) A widespread glutamine-sensing mechanism in the plant kingdom. *Cell*, 159(5), 1188–1199. Available from: https://doi.org/10.1016/j.cell.2014.10.015

Delauney, A.J., Hu, C.A., Kishor, P.B. & Verma, D.P. (1993) Cloning of ornithine delta-aminotransferase cDNA from *Vigna aconitifolia* by trans-complementation in *Escherichia coli* and regulation of proline biosynthesis. *Journal of Biological Chemistry*, 268(25), 18673–18678.

Delauney, A.J. & Verma, D.P.S. (1993) Proline biosynthesis and osmoregulation in plants. *The Plant Journal*, 4(2), 215–223. Available from: https://doi.org/10.1046/j.1365-313X.1993.04020215.x

Deuschle, K., Funck, D., Forlani, G., Stransky, H., Biehl, A., Leister, D. et al. (2004) The role of Δ^1-pyrroline-5-carboxylate dehydrogenase in proline degradation. *The Plant Cell*, 16(12), 3413–3425. Available from: https://doi.org/10.1105/tpc.104.023622

Díaz, P., Betti, M., Sánchez, D.H., Udvardi, M.K., Monza, J. & Márquez, A.J. (2010) Deficiency in plastidic glutamine synthetase alters proline metabolism and transcriptomic response in *Lotus japonicus* under drought stress. *New Phytologist*, 188(4), 1001–1013. Available from: https://doi.org/10.1111/j.1469-8137.2010.03440.x

Fichman, Y., Gerdes, S.Y., Kovács, H., Szabados, L., Zilberstein, A. & Csonka, L.N. (2015) Evolution of proline biosynthesis: enzymology, bioinformatics, genetics, and transcriptional regulation. *Biological Reviews*, 90(4), 1065–1099. Available from: https://doi.org/10.1111/brv.12146

Forlani, G., Berlicki, Ł., Duò, M., Dziędzioła, G., Giberti, S., Bertazzini, M. et al. (2013) Synthesis and evaluation of effective inhibitors of plant δ^1-pyrroline-5-carboxylate reductase. *Journal of Agricultural and Food Chemistry*, 61(28), 6792–6798. Available from: https://doi.org/10.1021/jf401234s

Forlani, G., Bertazzini, M. & Cagnano, G. (2019) Stress-driven increase in proline levels, and not proline levels themselves, correlates with the

ability to withstand excess salt in a group of 17 Italian rice genotypes. *Plant Biology*, 21(2), 336–342. Available from: https://doi.org/10.1111/plb.12916

Forlani, G., Bertazzini, M. & Giberti, S. (2014) Differential accumulation of γ-aminobutyric acid in elicited cells of two rice cultivars showing contrasting sensitivity to the blast pathogen. *Plant Biology*, 16(6), 1127–1132. Available from: https://doi.org/10.1111/plb.12165

Forlani, G., Bertazzini, M., Zarattini, M. & Funck, D. (2015) Functional characterization and expression analysis of rice δ^1-pyrroline-5-carboxylate dehydrogenase provide new insight into the regulation of proline and arginine catabolism. *Frontiers in Plant Science*, 6, 591. Available from: https://doi.org/10.3389/fpls.2015.00591

Forlani, G., Bertazzini, M., Zarattini, M., Funck, D., Ruszkowski, M. & Nocek, B. (2015) Functional properties and structural characterization of rice δ^1-pyrroline-5-carboxylate reductase. *Frontiers in Plant Science*, 6, 565. Available from: https://doi.org/10.3389/fpls.2015.00565

Forlani, G. & Funck, D. (2020) A specific and sensitive enzymatic assay for the quantitation of L-proline. *Frontiers in Plant Science*, 11, 582026. Available from: https://doi.org/10.3389/fpls.2020.582026

Forlani, G., Giberti, S. & Doria, E. (2023) The levels of DAHP synthase, the first enzyme of the shikimate pathway, are related to free aromatic amino acids and glutamine content in *Nicotiana plumbaginifolia* cell cultures. *Plants*, 12(13), 2524. Available from: https://doi.org/10.3390/plants12132524

Forlani, G., Makarova, K.S., Ruszkowski, M., Bertazzini, M. & Nocek, B. (2015) Evolution of plant δ^1-pyrroline-5-carboxylate reductases from phylogenetic and structural perspectives. *Frontiers in Plant Science*, 6, 567. Available from: https://doi.org/10.3389/fpls.2015.00567

Forlani, G., Trovato, M., Funck, D. & Signorelli, S. (2019) Regulation of proline accumulation and its molecular and physiological functions in stress defence. In: Hossain, M.A., Kumar, V., Burritt, D.J., Fujita, M. & Mäkelä, P.S.A. (Eds.) *Osmoprotectant-mediated abiotic stress tolerance in plants: recent advances and future perspectives*. Cham: Springer International Publishing, pp. 73–97.

Funck, D., Baumgarten, L., Stift, M., von Wirén, N. & Schönemann, L. (2020) Differential contribution of P5CS isoforms to stress tolerance in Arabidopsis. *Frontiers in Plant Science*, 11, 565134. Available from: https://doi.org/10.3389/fpls.2020.565134

Funck, D., Sinn, M., Forlani, G. & Hartig, J.S. (2023) Guanidine production by plant homoarginine-6-hydroxylases. *eLife*, 12, RP91458. Available from: https://doi.org/10.7554/elife.91458.1

Funck, D., Stadelhofer, B. & Koch, W. (2008) Ornithine-δ-aminotransferase is essential for arginine catabolism but not for proline biosynthesis. *BMC Plant Biology*, 8, 40. Available from: https://doi.org/10.1186/1471-2229-8-40

Funck, D., Winter, G., Baumgarten, L. & Forlani, G. (2012) Requirement of proline synthesis during Arabidopsis reproductive development. *BMC Plant Biology*, 12, 191. Available from: https://doi.org/10.1186/1471-2229-12-191

Gent, L. & Forde, B.G. (2017) How do plants sense their nitrogen status? *Journal of Experimental Botany*, 68(10), 2531–2539. Available from: https://doi.org/10.1093/jxb/erx013

Ghosh, U.K., Islam, M.N., Siddiqui, M.N. & Khan, M.A.R. (2021) Understanding the roles of osmolytes for acclimatizing plants to changing environment: a review of potential mechanism. *Plant Signaling & Behavior*, 16(8), 1913306. Available from: https://doi.org/10.1080/15592324.2021.1913306

Giberti, S., Funck, D. & Forlani, G. (2014) Δ^1-pyrroline-5-carboxylate reductase from *Arabidopsis thaliana*: stimulation or inhibition by chloride ions and feedback regulation by proline depend on whether NADPH or NADH acts as co-substrate. *New Phytologist*, 202(3), 911–919. Available from: https://doi.org/10.1111/nph.12701

Giberti, S., Bertazzini, M., Liboni, M., Berlicki, L., Kafarski, P., & Forlani, G. (2017). Phytotoxicity of aminobisphosphonates targeting both delta (1)-pyrroline-5-carboxylate reductase and glutamine synthetase. *Pest Management Science*, 73(2), 435–443. https://doi.org/10.1002/ps.4299

Hare, P.D. & Cress, W.A. (1997) Metabolic implications of stress-induced proline accumulation in plants. *Plant Growth Regulation*, 21(2), 79–102. Available from: https://doi.org/10.1023/A:1005703923347

Hayat, S., Hayat, Q., Alyemeni, M.N., Wani, A.S., Pichtel, J. & Ahmad, A. (2012) Role of proline under changing environments: a review. *Plant Signaling & Behavior*, 7(11), 1456–1466. Available from: https://doi.org/10.4161/psb.21949

Hu, C.A., Delauney, A.J. & Verma, D.P. (1992) A bifunctional enzyme (delta 1-pyrroline-5-carboxylate synthetase) catalyzes the first two steps in proline biosynthesis in plants. *Proceedings of the National Academy of Sciences of the United States of America*, 89(19), 9354–9358. Available from: https://doi.org/10.1073/pnas.89.19.9354

Hu, C.A., Lin, W.W., Obie, C. & Valle, D. (1999) Molecular enzymology of mammalian Δ^1-pyrroline-5-carboxylate synthase. *Journal of Biological Chemistry*, 274(10), 6754–6762. Available from: https://doi.org/10.1074/jbc.274.10.6754

Ishizaki, T., Ohsumi, C., Totsuka, K. & Igarashi, D. (2010) Analysis of glutamate homeostasis by overexpression of *Fd-GOGAT* gene in *Arabidopsis thaliana*. *Amino Acids*, 38(3), 943–950. Available from: https://doi.org/10.1007/s00726-009-0303-2

Liang, C., Zhang, Y., Cheng, S., Osorio, S., Sun, Y., Fernie, A.R. et al. (2015) Impacts of high ATP supply from chloroplasts and mitochondria on the leaf metabolism of *Arabidopsis thaliana*. *Frontiers in Plant Science*, 6, 922. Available from: https://doi.org/10.3389/fpls.2015.00922

Mattioli, R., Biancucci, M., Lonoce, C., Costantino, P. & Trovato, M. (2012) Proline is required for male gametophyte development in Arabidopsis. *BMC Plant Biology*, 12, 236. Available from: https://doi.org/10.1186/1471-2229-12-236

Monteoliva, M.I., Rizzi, Y.S., Cecchini, N.M., Hajirezaei, M.R. & Alvarez, M.E. (2014) Context of action of proline dehydrogenase (ProDH) in the hypersensitive response of Arabidopsis. *BMC Plant Biology*, 14, 21. Available from: https://doi.org/10.1186/1471-2229-14-21

Nordin, A. & Näsholm, T. (1997) Nitrogen storage forms in nine boreal understorey plant species. *Oecologia*, 110(4), 487–492. Available from: https://doi.org/10.1007/s004420050184

Pérez-Arellano, I., Rubio, V. & Cervera, J. (2005) Dissection of *Escherichia coli* glutamate 5-kinase: functional impact of the deletion of the PUA domain. *FEBS Letters*, 579(30), 6903–6908. Available from: https://doi.org/10.1016/j.febslet.2005.11.037

Pérez-Arellano, I., Carmona-Álvarez, F., Gallego, J. & Cervera, J. (2010) Molecular mechanisms modulating glutamate kinase activity. Identification of the proline feedback inhibitor binding site. *Journal of Molecular Biology*, 404(5), 890–901. Available from: https://doi.org/10.1016/j.jmb.2010.10.019

Pérez-Arellano, I., Rubio, V. & Cervera, J. (2006) Mapping active site residues in glutamate-5-kinase. The substrate glutamate and the feed-back inhibitor proline bind at overlapping sites. *FEBS Letters*, 580(26), 6247–6253. Available from: https://doi.org/10.1016/j.febslet.2006.10.031

Qamar, A. (2015) Role of proline and pyrroline-5-carboxylate metabolism in plant defense against invading pathogens. *Frontiers in Plant Science*, 6, 503. Available from: https://doi.org/10.3389/fpls.2015.00503

Queval, G. & Noctor, G. (2007) A plate reader method for the measurement of NAD, NADP, glutathione, and ascorbate in tissue extracts: application to redox profiling during Arabidopsis rosette development. *Analytical Biochemistry*, 363(1), 58–69. Available from: https://doi.org/10.1016/j.ab.2007.01.005

Rai, A.N. & Penna, S. (2013) Molecular evolution of plant P5CS gene involved in proline biosynthesis. *Molecular Biology Reports*, 40(11), 6429–6435. Available from: https://doi.org/10.1007/s11033-013-2757-2

Raza, A., Razzaq, A., Mehmood, S., Zou, X., Zhang, X., Lv, Y. et al. (2019) Impact of climate change on crops adaptation and strategies to

tackle its outcome: a review. *Plants*, 8(2), 34. Available from: https://doi.org/10.3390/plants8020034

Sabbioni, G., Funck, D. & Forlani, G. (2021) Enzymology and regulation of δ^1-pyrroline-5-carboxylate synthetase 2 from rice. *Frontiers in Plant Science*, 12, 672702. Available from: https://doi.org/10.3389/fpls.2021.672702

Scharte, J., Hassa, S., Herrfurth, C., Feussner, I., Forlani, G., Weis, E. et al. (2023) Metabolic priming in G6PDH isoenzyme-replaced tobacco lines improves stress tolerance and seed yields via altering assimilate partitioning. *The Plant Journal*, 116, 1696–1716. Available from: https://doi.org/10.1111/tpj.16460

Sekine, T., Kawaguchi, A., Hamano, Y. & Takagi, H. (2007) Desensitization of feedback inhibition of thesaccharomyces cerevisiaeγ-glutamyl kinase enhances proline accumulation and freezing tolerance. *Applied and Environmental Microbiology*, 73(12), 4011–4019. Available from: https://doi.org/10.1128/aem.00730-07

Sharma, S., Villamor, J.G. & Verslues, P.E. (2011) Essential role of tissue-specific proline synthesis and catabolism in growth and redox balance at low water potential. *Plant Physiology*, 157(1), 292–304. Available from: https://doi.org/10.1104/pp.111.183210

Shinde, S., Villamor, J.G., Lin, W.D., Sharma, S. & Verslues, P.E. (2016) Proline coordination with fatty acid synthesis and redox metabolism of chloroplast and mitochondria. *Plant Physiology*, 172(2), 1074–1088. Available from: https://doi.org/10.1104/pp.16.01097

Strizhov, N., Ábrahám, E., Ökrész, L., Blickling, S., Zilberstein, A., Schell, J. et al. (1997) Differential expression of two P5CS genes controlling proline accumulation during salt-stress requires ABA and is regulated by ABA1, ABI1 and AXR2 in Arabidopsis. *The Plant Journal*, 12(3), 557–569. Available from: https://doi.org/10.1046/j.1365-313X.1997.00537.x

Székely, G., Ábrahám, E., Cséplő, Á., Rigó, G., Zsigmond, L., Csiszár, J. et al. (2008) Duplicated P5CS genes of Arabidopsis play distinct roles in stress regulation and developmental control of proline biosynthesis. *The Plant Journal*, 53(1), 11–28. Available from: https://doi.org/10.1111/j.1365-313X.2007.03318.x

Takahashi, H., Takahara, K., Hashida, S., Hirabayashi, T., Fujimori, T., Kawai-Yamada, M. et al. (2009) Pleiotropic modulation of carbon and nitrogen metabolism in Arabidopsis plants overexpressing the *NAD kinase2* gene. *Plant Physiology*, 151(1), 100–113. Available from: https://doi.org/10.1104/pp.109.140665

Trovato, M., Forlani, G., Signorelli, S. & Funck, D. (2019) Proline metabolism and its functions in development and stress tolerance. In: Hossain, M.A., Kumar, V., Burritt, D.J., Fujita, M. & Mäkelä, P.S.A. (Eds.) *Osmoprotectant-mediated abiotic stress tolerance in plants: recent advances and future perspectives*. Cham: Springer International Publishing, pp. 41–72.

Turchetto-Zolet, A.C., Margis-Pinheiro, M. & Margis, R. (2009) The evolution of pyrroline-5-carboxylate synthase in plants: a key enzyme in proline synthesis. *Molecular Genetics and Genomics*, 281(1), 87–97. Available from: https://doi.org/10.1007/s00438-008-0396-4

Verbruggen, N. & Hermans, C. (2008) Proline accumulation in plants: a review. *Amino Acids*, 35(4), 753–759. Available from: https://doi.org/10.1007/s00726-008-0061-6

Wang, X., Li, B.B., Ma, T.T., Sun, L.Y., Tai, L., Hu, C.H. et al. (2020) The NAD kinase OsNADK1 affects the intracellular redox balance and enhances the tolerance of rice to drought. *BMC Plant Biology*, 20(1), 11. Available from: https://doi.org/10.1186/s12870-019-2234-8

Winter, G., Todd, C.D., Trovato, M., Forlani, G. & Funck, D. (2015) Physiological implications of arginine metabolism in plants. *Frontiers in Plant Science*, 6, 534. Available from: https://doi.org/10.3389/fpls.2015.00534

Yang, Z., Zhao, X., Shang, W., Liu, Y., Ji, J.F., Liu, J.P. et al. (2021) Pyrroline-5-carboxylate synthase senses cellular stress and modulates metabolism by regulating mitochondrial respiration. *Cell Death & Differentiation*, 28(1), 303–319. Available from: https://doi.org/10.1038/s41418-020-0601-5

Zarattini, M. & Forlani, G. (2017) Toward unveiling the mechanisms for transcriptional regulation of proline biosynthesis in the plant cell response to biotic and abiotic stress conditions. *Frontiers in Plant Science*, 8, 927. Available from: https://doi.org/10.3389/fpls.2017.00927

Zhang, B., Tastan, Ö.Y., Zhou, X., Guo, C.J., Liu, X., Thind, A. et al. (2020) The proline synthesis enzyme P5CS forms cytoophidia in Drosophila. *Journal of Genetics and Genomics*, 47(3), 131–143. Available from: https://doi.org/10.1016/j.jgg.2020.02.005

Zhang, C., Lu, Q. & Verma, D.P.S. (1995) Removal of feedback inhibition of Δ^1-pyrroline-5-carboxylate synthetase, a bifunctional enzyme catalyzing the first two steps of proline biosynthesis in plants. *Journal of Biological Chemistry*, 270(35), 20491–20496. Available from: https://doi.org/10.1074/jbc.270.35.20491

Zhong, J., Guo, C.J., Zhou, X., Chang, C.C., Yin, B., Zhang, T. et al. (2022) Structural basis of dynamic P5CS filaments. *eLife*, 11, e76107. Available from: https://doi.org/10.7554/eLife.76107

SUPPORTING INFORMATION

Additional supporting information can be found online in the Supporting Information section at the end of this article.

How to cite this article: Forlani, G., Sabbioni, G., Barera, S. & Funck, D. (2024) A complex array of factors regulate the activity of *Arabidopsis thaliana* δ^1-pyrroline-5-carboxylate synthetase isoenzymes to ensure their specific role in plant cell metabolism. *Plant, Cell & Environment*, 47, 1348–1362. https://doi.org/10.1111/pce.14817